International Journal of Thermophysics, Vol. 12, No. 3, 1991

Thermodynamic Properties of 1,1,1,2-Tetrafluoroethane (R134a) in the Critical Region

S. Tang,[1] G. X. Jin,[1] and J. V. Sengers[1,2]

Received August 28, 1990

A theoretically based simplified crossover model, which is capable of representing the thermodynamic properties of fluids in a large range of temperatures and densities around the critical point, is presented. The model is used to predict the thermodynamic properties of R134a in the critical region from a limited amount of available experimental information. Values for various thermodynamic properties of R134a at densities from 2 to 8 mol · L^{-1} and at temperatures from 365 to 450 K are presented.

KEY WORDS: critical phenomena; equation of state; R134a; refrigerants; sound velocity; specific heat.

1. INTRODUCTION

As a stratospherically safe new refrigerant, 1,1,1,2-tetrafluoroethane (R134a) is considered to be a leading candidate to replace dichlorodifluoromethane (R12) as a working fluid in air-conditioning and refrigeration technology [1–4]. As a consequence it has become very important to obtain reliable information concerning the thermodynamic properties of R134a [5], and several research groups have recently reported experimental thermodynamic-property data for R134a [6–16]. The critical temperature of R134a is about 100°C. Most of the available experimental data pertain to the vapor and liquid phase of R134a. With the exception of some pressure [6, 7] and density [8] data, little information is available for the

[1] Institute for Physical Science and Technology, University of Maryland, College Park, Maryland 20742, U.S.A.

[2] Thermophysics Division, National Institute of Standards and Technology, Gaithersburg, Maryland 20899, U.S.A.

0195-928X/91/0500-0515$06.50/0

thermodynamic properties of R134a in the critical region. It is known that thermodynamic properties like the compressibility and the specific heat become large in a substantial range of temperatures and densities around the critical point [17]. In this paper we refer to the range where critical enhancements in the compressibility and specific heat are observed as the global critical region.

An interesting question is whether the thermodynamic properties of a fluid in the global critical region can be predicted from a limited amount of experimental information. Until recently, this question would have been answered negatively. Asymptotically close to the critical point the thermodynamic properties exhibit singular scaling-law behavior with known universal critical exponents and critical scaling functions [18, 19]. However, the range in temperatures and densities where the asymptotic singular behavior applies is quite small [20]. As a consequence one needs accurate experimental data very close to the critical point to determine the values of the system-dependent coefficients in the asymptotic scaling laws. Furthermore, even if this information is available, a knowledge of the asymptotic scaling laws is insufficient to represent the thermodynamic properties in the region relevant to technological applications, that is, in the global critical region. On the other hand, classical equations, like those used for R134a, to represent the thermodynamic properties far away from the critical point [6, 7, 9, 21], cannot reliably be extrapolated into the critical region.

To address this problem one needs a theoretical description of the global behavior of the thermodynamic properties in the critical region that includes the nonasymptotic critical behavior and encompasses the crossover from singular thermodynamic behavior close to the critical point to regular thermodynamic behavior far away from the critical point [19]. The asymptotic scaled thermodynamic behavior can be derived on the basis of the Landau–Ginzburg–Wilson theory of critical phenomena [18]. This theory elucidates how the effects of critical fluctuations on the thermodynamic properties can be accounted for by a renormalization procedure. Several investigators have made attempts to extend the Landau–Ginzburg–Wilson theory to a theory for the global critical behavior of the thermodynamic properties [22–32]. Very recently our group has been able to use this approach so as to obtain an actual theoretically based equation of state that is capable of representing the thermodynamic properties of fluids in the global critical region [33]. It is the purpose of the present paper to demonstrate how this new theoretical equation of state can be used to determine the thermodynamic properties of an important technical fluid like R134a from a limited amount of available experimental data.

2. SIMPLIFIED CROSSOVER MODEL FOR THE CRITICAL REGION

Let T be the temperature, P the pressure, ρ the density, μ the chemical potential, and a the specific Helmholtz free energy, i.e., the Helmholtz free energy per unit *mass*. We use the critical temperature T_c, the critical pressure P_c, and the critical density ρ_c to define dimensionless properties as

$$\tilde{T} = -\frac{T_c}{T}, \qquad \tilde{\rho} = \frac{\rho}{\rho_c}, \qquad \tilde{\mu} = \frac{\rho_c T_c}{P_c} \cdot \frac{\mu}{T}, \qquad \tilde{A} = \frac{T_c}{P_c} \cdot \frac{\rho a}{T} \tag{1}$$

In addition, we introduce

$$\Delta\tilde{T} = \tilde{T} + 1, \qquad \Delta\tilde{\rho} = \tilde{\rho} - 1, \qquad \Delta\tilde{\mu} = \tilde{\mu} - \mu_0(\tilde{T}) \tag{2}$$

where $\tilde{\mu}_0(\tilde{T})$ is an analytic background function such that $\Delta\tilde{\mu} = 0$ at the critical point. $\tilde{A}$ is a reduced Helmholtz free-energy density, i.e., a reduced Helmholtz free energy per unit *volume* [34]. To characterize the dependence of this Helmholtz free-energy density as a function of temperature and density in the critical region, it is decomposed as

$$\tilde{A} = \Delta\tilde{A} + \tilde{\rho}\tilde{\mu}_0(\tilde{T}) + \tilde{A}_0(\tilde{T}) \tag{3}$$

where $\tilde{A}_0(\tilde{T})$ is another analytic background function such that $\tilde{A}_0 = -1$ at the critical temperature.

The term $\Delta\tilde{A}$ in Eq. (3) contains the effect of critical fluctuations and it is this term which becomes singular at the critical point. In the classical mean-field theory $\Delta\tilde{A}$ can be represented by an analytic Landau expansion of the form [33]

$$\Delta\tilde{A}_{mf} = \frac{1}{2} tM^2 + \frac{1}{4!} u\Lambda M^4 + \frac{1}{5!} a_{05} M^5 + \frac{1}{6!} a_{06} M^6 + \frac{1}{4!} a_{14} tM^4 + \frac{1}{2!\,2!} a_{22} t^2 M^2 \tag{4}$$

where u, Λ, a_{05}, a_{06}, a_{14}, and a_{22} are system-dependent coefficients and where the temperature-like variable t and the order-parameter M are related to $\Delta\tilde{T}$ and $\Delta\tilde{\rho}$ by the transformation

$$t = c_t \Delta\tilde{T}, \qquad M = c_\rho(\Delta\tilde{\rho} - d_1 \Delta\tilde{T}) \tag{5}$$

and where c_t, c_ρ, and d_1 are additional system-dependent coefficients. A term proportional to tM^3 does not need to be included in Eq. (4) since it

can be eliminated by a transformation of variables [35]. In principle, the Landau expansion contains an arbitrary number of terms, but for our purpose we terminate the expansion after six terms.

As shown by Chen et al. [33] in a previous publication, the renormalized $\Delta\tilde{A}$, incorporating the effects of critical fluctuations, can be obtained from Eq. (4) by the following transformation:

(i) replace the variable t by $t\mathscr{T}\mathscr{U}^{-1/2}$,

(ii) replace the variable M in the even terms by $M\mathscr{D}^{1/2}\mathscr{U}^{1/4}$ and replace the variable in the odd M^5 term by $M\mathscr{D}^{1/2}\mathscr{V}^{1/5}\mathscr{U}^{1/5}$, and

(iii) add a nonscaling fluctuation-induced contribution of the form $-\frac{1}{2}t^2\mathscr{K}$.

The new functions in this transformation are defined as

$$\mathscr{T} = Y^{(2-\nu^{-1})/\omega}, \qquad \mathscr{U} = Y^{1/\omega}, \qquad \mathscr{D} = Y^{-\eta/\omega},$$
$$\mathscr{V} = Y^{(\omega_a - 1/2)/\omega}, \qquad \mathscr{K} = \frac{\nu}{\alpha\bar{u}\Lambda}(Y^{-\alpha/\omega\nu} - 1) \tag{6}$$

where ν, η, and $\alpha = 2 - 3\nu$ are the usual critical exponents [19, 36], ω and ω_a are the symmetric and asymmetric correction-to-scaling exponents [19, 37], and $\bar{u}$ is defined as

$$\bar{u} = u/u^* \tag{7}$$

in terms of the fixed-point coupling constant u^* [27, 33, 38]. The critical exponents ν, η, α, ω, and ω_a and the coupling constant u^* are universal. For fluids they have the values corresponding to three-dimensional systems with short-range forces and a scalar order parameter, often referred to as Ising-like systems [19]. The values of these universal critical-region constants are given in Table I. The crossover function Y in Eq. (6) is to be determined from [33]

$$1 + (\bar{u} - 1)Y = \bar{u}\left(1 + \frac{\Lambda^2}{\kappa^2}\right)^{1/2} Y^{1/\omega} \tag{8}$$

Table I. Universal Critical-Region Constants

$\nu = 0.630$
$\eta = 0.0333$
$\alpha = 2 - 3\nu = 0.110$
$\omega = 0.51/\nu = 0.80952$
$\omega_a = 2.1$
$u^* = 0.472$

with

$$\kappa^2 = t\mathscr{T} + \tfrac{1}{2}u^*\bar{u}\Lambda M^2\mathscr{D}\mathscr{U} \tag{9}$$

After application of the above transformation to the Landau expansion given by Eq. (4) the renormalized $\Delta\tilde{A}$ is obtained as [33, 39]

$$\Delta\tilde{A} = \frac{1}{2}tM^2\mathscr{T}\mathscr{D} + \frac{1}{4!}u^*\bar{u}\Lambda M^4\mathscr{D}^2\mathscr{U} + \frac{1}{5!}a_{05}M^5\mathscr{D}^{5/2}\mathscr{V}\mathscr{U} + \frac{1}{6!}a_{06}M^6\mathscr{D}^3\mathscr{U}^{3/2}$$
$$+ \frac{1}{4!}a_{14}tM^4\mathscr{T}\mathscr{D}^2\mathscr{U}^{1/2} + \frac{1}{2!\,2!}a_{22}t^2M^2\mathscr{T}^2\mathscr{D}\mathscr{U}^{-1/2} - \frac{1}{2}t^2\mathscr{K} \tag{10}$$

The variable κ, defined by Eq. (9), serves as a measure of the distance from the critical point. As $\kappa \to 0$, $Y \to 0$ and one recovers from Eq. (10) the scaled asymptotic critical behavior. As $\kappa \to \infty$, $Y \to 1$ and Eq. (10) reduces to the classical Landau expansion given by Eq. (4).

To specify the total Helmholtz free-energy density $\tilde{A}$, defined by Eq. (3), we represent the analytic background functions $\tilde{A}_0(\tilde{T})$ and $\tilde{\mu}_0(\tilde{T})$ by truncated Taylor expansions [32, 33]

$$\tilde{A}_0(\tilde{T}) = -1 + \sum_{j=1}^{4} \tilde{A}_j(\Delta\tilde{T})^j \tag{11}$$

$$\tilde{\mu}_0(\tilde{T}) = \sum_{j=0}^{3} \tilde{\mu}_j(\Delta\tilde{T})^j \tag{12}$$

where $\tilde{A}_j$ and $\tilde{\mu}_j$ are system-dependent coefficients.

Unlike the three-dimensional Ising model, a fluid near the vapor–liquid critical point is asymmetric in the order parameter M. This asymmetry is reflected in the presence of a term proportional to M^5 in the Landau expansion, Eq. (4), and by the presence of an additional term $d_1\Delta\tilde{T}$ in the relation (5) between M and $\Delta\tilde{T}$. The theory predicts that the asymmetry also induces an additional mixing transformation of the form [32, 33, 35]

$$t = c_t\Delta\tilde{T} + c\left(\frac{\partial\,\Delta\tilde{A}}{\partial M}\right)_t, \qquad M = c_\rho(\Delta\tilde{\rho} - d_1\Delta\tilde{T}) + c\left(\frac{\partial\,\Delta\tilde{A}}{\partial t}\right)_M \tag{13}$$

where the coefficient c is a measure of the magnitude of the mixing transformation. In practice, however, we find that the effect of mixing is quite small for simple fluids, except for a strongly asymmetric fluid like steam [33]. For R134a an equally good representation of the available experimental information is obtained with $c = 0$. An added advantage is that setting $c = 0$ greatly simplifies the fundamental equation for $\tilde{A}$. In this

paper we therefore use the simplified crossover model given by Eq. (10) with $c = 0$. Equation (10) with Eqs. (11) and (12) completely specifies our simplified crossover model. The corresponding equations for the various derived thermodynamic properties are obtained from those presented in Ref. 33 with $c = 0$.

In the previous work of our research group the thermodynamic properties of fluids in the vicinity of the critical point were represented by a so-called revised and extended parametric equation of state [40–42]. As documented elsewhere [39], the range of validity of the crossover model used here is much larger than that of the revised and extended parametric equation of state and yields an accurate representation of the thermodynamic properties in essentially the entire global critical region [33]. An added advantage, explored in the present paper, is that the system-dependent coefficients in the new equation of state can be determined from experimental information, even if little of it is inside the range of asymptotic critical scaling behavior.

3. APPLICATION TO R134a

In order to apply our crossover model we first need the critical parameters T_c, ρ_c, and P_c. Values for the critical parameters of R134a as reported by a number of investigators are listed in Table II. For our purpose it is important that the values of the critical parameters adopted be consistent with other experimental thermodynamic-property data in the near-vicinity of the critical point. The only available information of this nature is the saturated vapor and liquid densities reported by Kabata et al. [8]. We therefore selected $T_c = 374.30$ K and $\rho_c = 5.050$ mol · L^{-1}, which we found to be consistent with the coexisting density data of Kabata et al., even though Kabata et al. quoted a lower value for ρ_c; the critical pressure

Table II. Critical Parameters Reported for R134a

Reference	T_c (K)	ρ_c (mol · L^{-1})	P_c (MPa)
Basu and Wilson [7]	374.25 ± 0.15	5.020 ± 0.05	4.067 ± 0.003
Kabata et al. [8]	374.30 ± 0.01	4.979 ± 0.03	
Kubota et al. [10]	374.25		4.065
McLinden et al. [11]	374.205 ± 0.01	5.051 ± 0.01	4.056 ± 0.01
Morrison and Ward [15]	374.205	5.050	4.068
This work	374.30	5.050	4.065

$P_c = 4.065$ MPa was subsequently selected as providing the best fit to the available P–ρ–T data as discussed below.

In addition to the critical parameters the crossover model contains the following system-dependent constants: the crossover constants $\bar{u}$ and Λ, the coefficients c_t, c_ρ, and d_1 in the expressions for the scaling fields, the classical coefficients a_{ij}, the coefficients $\tilde{A}_j$ in the background contribution to the equation of state, and the coefficients $\tilde{\mu}_j$ in the background contribution to the caloric properties. With the exception of the caloric background coefficients $\tilde{\mu}_j$, they can be determined from a fit to experimental P–ρ–T data [33]. Since for R134a most of the available P–ρ–T data are not asymptotically close to the critical point, we applied our crossover model in as large a range of temperatures and densities as possible, where an acceptable representation could be obtained. This range is indicated by the shaded area in Fig. 1. The most accurate P–ρ–T data for R134a are those reported by Weber [9], but they cover the gas phase up to a density of 2.33 mol · L^{-1} only, which is still well below the critical density of 5.05 mol · L^{-1}. We therefore determined the system-dependent parameters in the equation of state from a fit to the more comprehensive set of pressure data from Piao et al. [12], supplemented with pressure data from Weber [9] to the extent they are inside the range shown in Fig. 1. The values obtained for the system-dependent coefficients are presented in Table III. With the error estimates assigned by the experimenters [9, 12], the combined set of pressure data (94 data from Piao et al. and 22 data

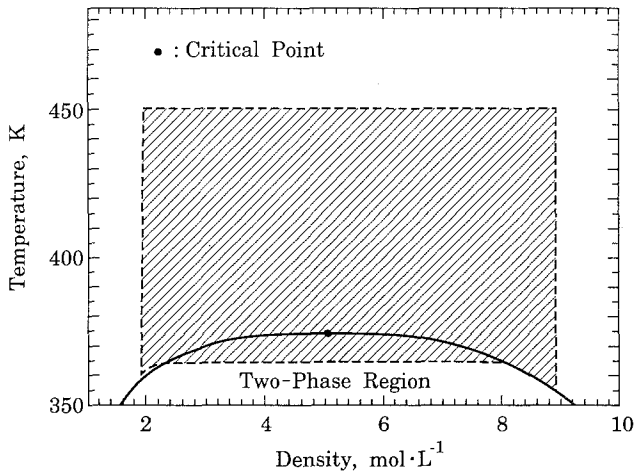

Fig. 1. Range of temperatures and densities of our crossover model for R134a as indicated by the shaded area. The solid curve represents the two-phase boundary.

Table III. System-Dependent Constants in Simplified Crossover Model for R134a[a]

Critical parameters
$P_c = 4.065$ MPa, $T_c = 374.30$ K, $\rho_c = 5.050$ mol · L^{-1}

Crossover parameters
$\bar{u} = 0.44970$, $\Lambda = 2.3165$

Scaling-field parameters
$c_t = 2.7165$, $c_\rho = 2.2741$, $d_1 = -0.21192$

Classical parameters
$a_{05} = -1.5021$, $a_{06} = 2.1487$, $a_{14} = 0.33807$, $a_{22} = 0.17213$

P–ρ–T background parameters
$\tilde{A}_1 = -6.6526$, $\tilde{A}_2 = 3.5463$, $\tilde{A}_3 = -3.9632$, $\tilde{A}_4 = 25.431$

Caloric background parameters
$\tilde{\mu}_0 = 2.5673$, $\tilde{\mu}_1 = 12.250$, $\tilde{\mu}_2 = -28.939$, $\tilde{\mu}_3 = -25.272$

[a] 1 mol · L^{-1} = 102.03 kg · m^{-3}.

from Weber) are reproduced with a reduced chi-square of 5.5. This value of chi-square is larger than unity, but some relevant comments can be made. First, there are differences in the pressure data from Piao et al. and from Weber up to about twice the estimated error, indicating that the actual errors may be slightly larger (Fig. 2). Second, a comparison can also be made with pressure data reported by Basu and Wilson [7] which were not used in the fit. With $\sigma_P = 0.1\%$, $\sigma_T = 0.03$ K, and $\sigma_\rho = 0.08\%$ as claimed by Basu and Wilson [7], their 29 data points inside the range considered are reproduced with a reduced chi-square of 3.7, comparable to that obtained previously for carbon dioxide in a range of temperatures and densities somewhat smaller than that adopted here [33]. The actual deviations of the experimental pressure data are shown in Figs. 2 and 3. A comparison of the vapor pressures as calculated from our crossover model with experimental vapor-pressure data reported by Basu and Wilson [7], Weber [9], Kubota et al. [10], Piao et al. [12], and Morrison and Ward [15] is presented in Fig. 4.

As indicated in Fig. 1, the range of our crossover model corresponds to densities from 1.9 to 8.9 mol · L^{-1} and temperatures from 364.7 to 450 K. Below 364.7 K the crossover model can still be used in a small range but not at densities very close to the vapor phase boundary. We believe that this limitation is due to the approximate nature of Eq. (9) adopted for the variable κ^2. Attempts to extend our crossover model to lower temperatures near the phase boundary will be made in the future.

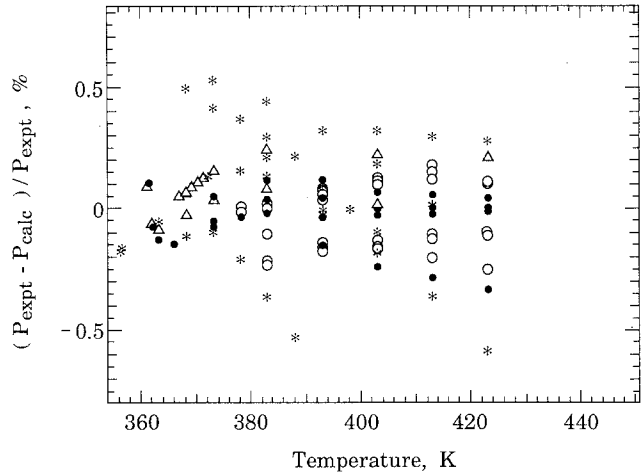

Fig. 2. Percentage deviations of the experimental pressures obtained by Weber (△, $\rho = 1.93$ mol · L^{-1} and $\rho = 2.33$ mol · L^{-1}) and by Piao et al. (●, $\rho = 1.99$–3.72 mol · L^{-1}; ○, $\rho = 4.50$–4.99 mol · L^{-1}; *, $\rho = 5.77$–8.87 mol · L^{-1}) from the values calculated with our crossover model.

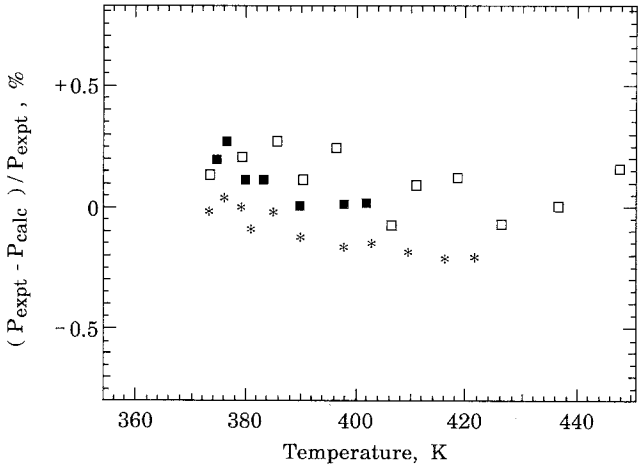

Fig. 3. Percentage deviations of the experimental pressures obtained by Basu and Wilson (□, $\rho = 2.56$ mol · L^{-1}; *, $\rho = 3.5$ mol · L^{-1}; ■, $\rho = 5.1$ mol · L^{-1}) from the values calculated with our crossover model.

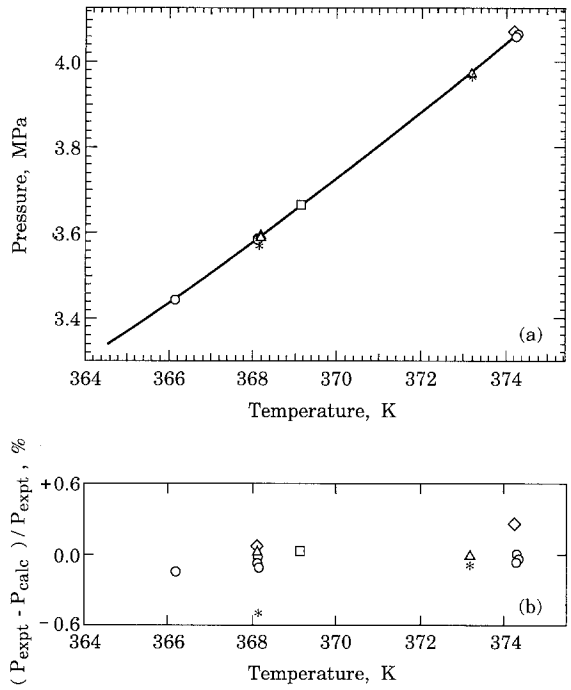

Fig. 4. (a) The vapor pressures of R134a as a function of temperature. The solid curves represent the vapor pressure as calculated from our crossover model. The data points are those reported by Basu and Wilson (□), Weber (△), Kubota et al. (*), Piao et al. (○), and Morrison and Ward (◇). (b) Percentage deviations of the experimental vapor pressures from the calculated vapor pressures.

In order to specify the Helmholtz free-energy density completely, specifically to calculate caloric properties, we need also values for the coefficients $\tilde{\mu}_j$ in Eq. (12). The coefficients $\tilde{\mu}_0$ and $\tilde{\mu}_1$ are related to the zero points of entropy and energy and are, therefore, arbitrary. To determine the coefficients μ_j for $j \geqslant 2$, we need some information about caloric properties as a function of temperature. The only available information of this nature is the sound-velocity data obtained by Guedes and Zollweg [43]. However, there is only one isotherm inside the range shown in Fig. 1 with some additional data in the liquid at 360 K. Previous experience indicates that to obtain a high accuracy, we need to retain terms in Eq. (12) up to at least $j=4$ [33]. However, the sound-velocity data of Guedes and Zollweg do not cover the critical region sufficiently to determine three coefficients μ_2, μ_3, and μ_4. Hence, we terminate the expansion (12) for $\tilde{\mu}_0(\tilde{T})$

at $j=3$, i.e., we approximate the background contribution to the specific heat by a linear function of reduced temperature. The values obtained for $\tilde{\mu}_2$ and $\tilde{\mu}_3$ are included in Table III.

In Fig. 5 we show the sound velocity as a function of pressures at a number of selected temperatures. The solid curves represent the values of the sound velocity as calculated from our crossover model. It can be seen that the agreement with the sound velocity data of Guedes and Zollweg is excellent, even at the low temperature of 360 K. The speed of sound as a function of pressure or density is known to exhibit a minimum inside the critical region. Guedes and Zollweg did not approach the vicinity of the critical point where these minima can be observed. Our crossover model gives definite predictions of the pressures and temperatures where these minima occur.

Saitoh et al. [13] recently reported experimental data for the isobaric specific heat c_p of R134a. The data are all in the liquid phase, but one point at $T=356$ K happens to lie just a little bit outside the range shown in Fig. 1. In Fig. 6 we show c_p of the liquid at 356 K as a function of pressure. As can be seen from this figure, our crossover model is in excellent agreement with this experimental value for c_p.

Having verified that our crossover model yields a satisfactory representation of the available experimental information that is not really very close to the critical point, what guarantee do we have that the crossover model will also yield reliable thermodynamic-property values in the

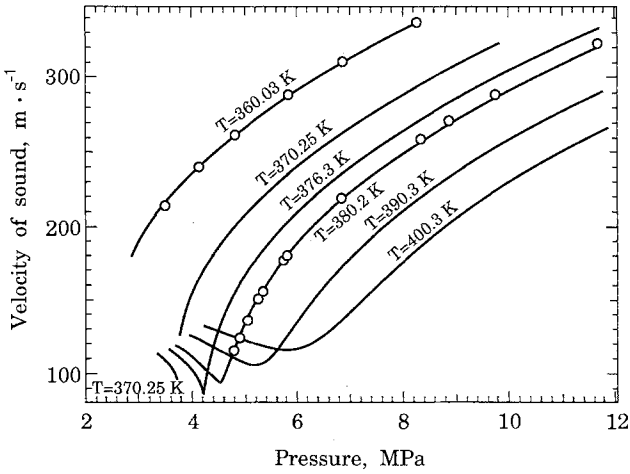

Fig. 5. The velocity of sound of R134a at selected temperatures as a function of pressure. The solid curves represent the values calculated from our crossover model. The circles indicate experimental data points obtained by Guedes and Zollweg [43].

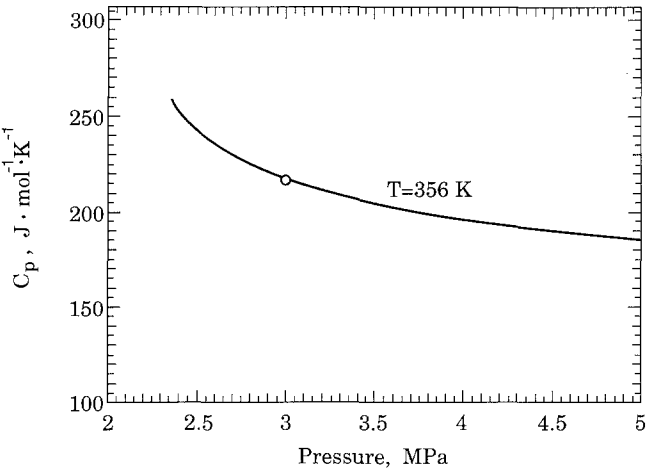

Fig. 6. The isobaric specific heat c_p of R134a in the liquid phase at $T = 356$ K as a function of pressure. The solid curve represents the values calculated from our crossover model. The circle indicates an experimental value reported by Saitoh et al. [13].

near-critical region where properties like the compressibility and specific heat become very large? As mentioned earlier, Kabata et al. [8] have reported experimental saturated vapor and liquid densities including at temperatures very close to the critical temperature. A comparison of the coexistence curve calculated from our crossover model with experimental data reported by Kabata et al. [8] as well as with some data points reported by Basu and Wilson [7], Piao et al. [12], Morrison and Ward [15], Weber [9], and Maezawa et al. [14] is presented in Fig. 7. Our crossover model is in very good agreement with the saturated vapor and liquid densities obtained by Kabata et al., although these data were not used in determining the coefficients in the model (except for fixing the *location* of the critical point as discussed in the beginning of this section).

Another check can be obtained by comparing the asymptotic behavior of our crossover model close to the critical point with the asymptotic power-law behavior of the surface tension. The principle of two-scale-factor universality specifies a universal relationship between the asymptotic behavior of the surface tension σ and that of the correlation length ξ, which in turn can be related to the asymptotic behavior of the specific heat. We use here this relationship in the form presented by Chaar et al. [44] and by Moldover and Rainwater [45], who introduced quantities $Y^{\pm}$ defined as

$$Y^{\pm} = \sigma[\alpha(\Delta\tilde{T})^2 \rho_c c_v^{\pm}/k_B]^{-2/3}/(k_B T_c) \tag{14}$$

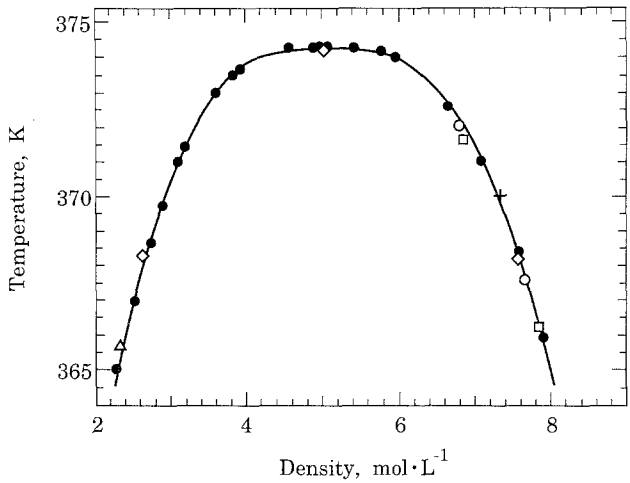

Fig. 7. The curve of coexisting vapor and liquid densities for R134a. The solid curve represents the coexistence curve as calculated from our crossover model. The data points indicate experimental values reported by Kabata et al. (●), Basu and Wilson (□), Piao et al. (○), Morrison and Ward (◇), Weber (△), and Maezawa et al. (+).

where c_v^+ and c_v^- are the asymptotic singular parts of the isochoric specific heat above and below the critical temperature, respectively, and where k_B is Boltzmann's constant. The quantities Y^+ and Y^- are universal. The available information has been reviewed by Chaar et al. [44] and Moldover and Rainwater [45], from which they conclude

$$Y^+ = 5.73 \pm 0.16, \qquad Y^- = 3.741 \pm 0.086 \tag{15}$$

The surface tension near the critical point goes asymptotically to zero as [46]

$$\sigma = \sigma_0 \, |\Delta \tilde{T}|^{2\nu} \tag{16}$$

while the specific heat per unit volume $\rho_c c_v^{\pm}$ diverges as [19]

$$\rho_c c_v^{\pm} = T_c^{-1} P_c \tilde{C}_0^{\pm} \, |\Delta \tilde{T}|^{-\alpha} \tag{17}$$

so that (14) can be rewritten in the form [44]

$$Y^{\pm} = \sigma_0 (\alpha P_c \tilde{C}_0^{\pm})^{-2/3} (k_B T_c)^{-1/3} \tag{18}$$

The surface tension of R134a has been measured by Chae et al. [47],

with the result $\sigma_0 = 0.0608\ \mathrm{N \cdot m^{-1}}$. The amplitude $\tilde{C}_0^+$ is obtained from our crossover model as

$$\tilde{C}_0^+ = \frac{\nu}{2\alpha}(2-\alpha)(1-\alpha)\, c_t^{2-\alpha}(\bar{u}\Lambda)^{2\alpha-1} \tag{19}$$

while $\tilde{C}_0^-$ is related to $\tilde{C}_0^+$ through the universal amplitude ratio [33]

$$\tilde{C}_0^+ / \tilde{C}_0^- = 0.502 \tag{20}$$

With the values of c_t, $\bar{u}$, and Λ found for R134a, we obtain $\tilde{C}_0^+ = 30.9$ and $\tilde{C}_0^- = 61.6$. Substitution of these values into Eq. (18) yields

$$Y^+ = 6.11, \qquad Y^- = 3.86 \tag{21}$$

to be compared with the universal values quoted in Eq. (15). While we do not reproduce the universal values (15) for Y^+ and Y^- exactly, we do obtain a reasonable approximation for Y^-. One should also note a possible uncertainty about the accuracy of the experimental surface-tension amplitude σ_0, since it was obtained by fitting Eq. (16) to the surface-tension data over a very large temperature range [47]. The major difference between Eq. (15) and Eq. (21) is a consequence of the fact that our crossover model implies a specific-heat amplitude ratio of 0.50 as given by Eq. (20), while there is evidence from the three-dimensional Ising model that this ratio is 0.52 [36].

It may also be interesting to note that the critical fluctuations not only lead to singular asymptotic critical behavior but also lead to a suppression of the critical temperature T_c from its classical value T_c' in the absence of fluctuations. For instance, by fitting the thermodynamic-property data of R134a to a simple classical Carnahan–Starling–De Santis equation, Morrison et al. find $T_c' = 386.7$ K [21, 48, 49]. The difference $T_c' - T_c \simeq 12°\mathrm{C}$ is thus a measure of the suppression of the critical temperature as a result of the long-range critical fluctuations.

4. RESULTS

Having verified the validity of our crossover model for the Helmholtz free-energy density of R134a to the extent that experimental data are available, we can compute all thermodynamic properties in the global critical region of R134a indicated in Fig. 1. However, before doing so we want to assign values to the coefficients $\tilde{\mu}_0$ and $\tilde{\mu}_1$ in Eq. (12) which are related to the zero points of entropy and energy. This is normally done by selecting a reference point at the boundary of the range of validity of the critical-region equation at a density and temperature sufficiently far away from the

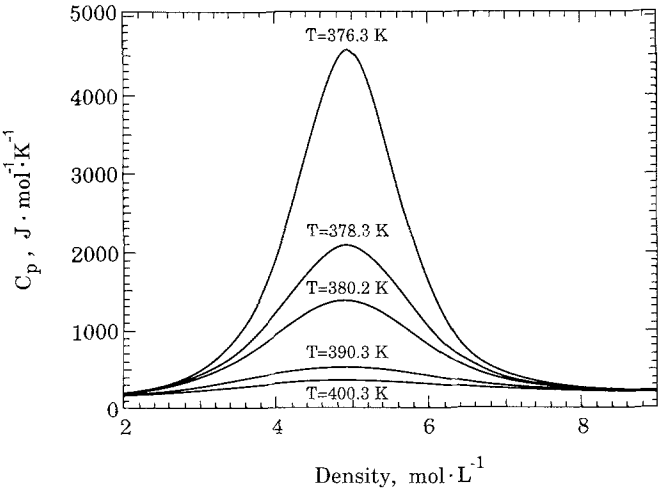

Fig. 8. The isobaric specific heat c_p, calculated from our crossover model for R134a, at selected temperatures as a function of density.

critical point; at this reference point the calculated entropy and enthalpy are then identified with the values calculated from a comprehensive equation which is preferably valid all the way down to the ideal-gas limit [40, 50]. Here we have selected as the reference point the point with $T = 373.15$ K (100°C) and $\rho = 1.9$ mol · L^{-1}, which is at the low-density side of the range of our crossover model. However, the comprehensive

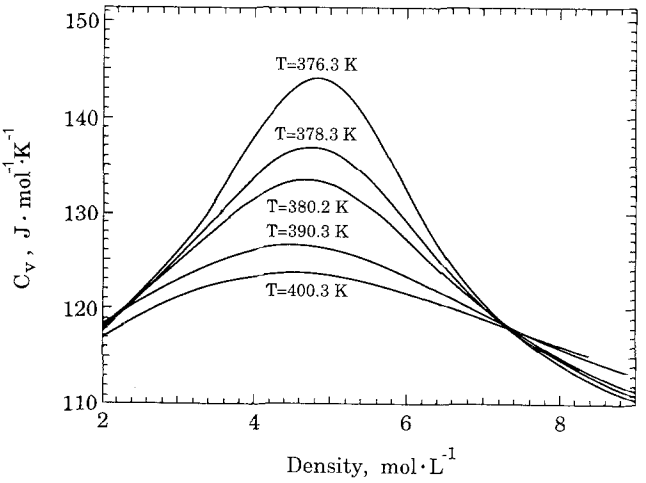

Fig. 9. The isochoric specific heat c_v, calculated from our crossover model for R134a, at selected temperatures as a function of density.

classical equations currently available for R134a [6, 7, 9, 21] are not very accurate. Hence, we prefer to calculate the specific-energy difference $u-u_r$ and the specific entropy difference $s-s_r$, where u_r and s_r are the specific energy and entropy at the reference point. This goal is obtained by selecting $\tilde{\mu}_0$ and $\tilde{\mu}_1$ so that $u_r=s_r=0$; these values of $\tilde{\mu}_0$ and $\tilde{\mu}_1$ are included in Table III.

In Table IV we present calculated values of the pressure P, the internal energy u, the entropy s, the enthalpy h, the isochoric specific heat c_v, the isobaric specific heat c_p, and the velocity of sound as a function of temperature and density. The behavior of c_p and c_v of R134a in the critical region is illustrated by isotherms shown in Figs. 8 and 9. Table V lists the saturation properties as a function of temperature, specifically the vapor pressure, the saturated vapor and liquid densities, and the latent heat.

From the information presented in Section 3, we conclude that our crossover model yields a reliable representation of the P–ρ–T surface of R134a in the global critical region. The equation of state also specifies the singular parts of the specific heats. The most serious approximation was introduced in approximating the background contribution to the specific heats by a linear function of temperature, since velocity-of-sound data did not permit us to establish the magnitude of higher-order terms in Eq. (12). As can be seen from Fig. 5, we have velocity-of-sound data at two temperatures only for determining the caloric background contribution. If more experimental information becomes available in the future, it is likely that some adjustments in this background contribution must be made at temperatures above 380 K, where no experimental information for any caloric property of R134a is currently available.

ACKNOWLEDGMENTS

We thank J. S. Gallagher, M. O. McLinden, G. Morrison, and L. A. Weber for stimulating discussions and for helping us with collecting the relevant information for R134a. We benefited from the expertise of A. Abbaci in handling crossover equations of state. We also are indebted to J. A. Zollweg for providing velocity-of-sound data prior to publication. The research was supported by the Division of Chemical Sciences of the Office of Basic Energy Sciences of the U.S. Department of Energy under Grant DE-FG05-88ER13902.

Table IV. Calculated Thermodynamic Properties

Temp. (K)	Density ($mol \cdot L^{-1}$)	Pressure (MPa)	Entropy ($J \cdot mol^{-1} \cdot K^{-1}$)	Energy ($J \cdot mol^{-1}$)	Enthalpy ($J \cdot mol^{-1}$)	C_v ($J \cdot mol^{-1} \cdot K^{-1}$)	C_p ($J \cdot mol^{-1} \cdot K^{-1}$)	Velocity of sound ($m \cdot s^{-1}$)	Phase region
365.0	2.0	3.243	−3.3	−1146.0	476	124	276	107.7	1
367.0	2.0	3.302	−2.7	−904.3	747	119	256	109.8	1
369.0	2.0	3.360	−2.0	−667.8	1012	118	244	111.5	1
371.0	2.0	3.418	−1.4	−432.8	1276	117	236	113.0	1
372.0	2.0	3.447	−1.1	−315.5	1408	117	232	113.7	1
373.0	2.0	3.475	−0.8	−198.2	1539	117	228	114.4	1
374.0	2.0	3.504	−0.5	−80.8	1671	117	225	115.1	1
375.0	2.0	3.532	−0.1	36.7	1803	118	222	115.8	1
376.0	2.0	3.561	0.2	154.3	1935	118	219	116.5	1
377.0	2.0	3.589	0.5	272.0	2066	118	217	117.1	1
379.0	2.0	3.645	1.1	507.8	2330	118	212	118.5	1
381.0	2.0	3.702	1.7	743.9	2595	118	208	119.8	1
383.0	2.0	3.757	2.3	980.4	2859	118	204	121.2	1
385.0	2.0	3.813	3.0	1217.1	3124	118	201	122.5	1
390.0	2.0	3.951	4.5	1809.0	3785	118	193	125.8	1
395.0	2.0	4.088	6.0	2399.6	4444	118	186	129.1	1
400.0	2.0	4.224	7.5	2986.8	5099	117	180	132.3	1
405.0	2.0	4.359	8.9	3568.8	5748	116	174	135.5	1
410.0	2.0	4.492	10.3	4143.9	6390	114	168	138.6	1
415.0	2.0	4.624	11.7	4710.7	7023	112	163	141.6	1
420.0	2.0	4.754	13.0	5267.8	7645	110	157	144.5	1
425.0	2.0	4.883	14.3	5814.0	8255	108	152	147.4	1
430.0	2.0	5.009	15.6	6348.6	8853	106	147	150.1	1
435.0	2.0	5.134	16.8	6870.5	9437	103	141	152.8	1
440.0	2.0	5.256	17.9	7379.2	10007	100	136	155.3	1
445.0	2.0	5.376	19.1	7874.1	10562	98	130	157.8	1
450.0	2.0	5.493	20.1	8354.7	11101	95	125	160.1	1

Table IV. *(Continued)*

Temp. (K)	Density ($mol \cdot L^{-1}$)	Pressure (MPa)	Entropy ($J \cdot mol^{-1} \cdot K^{-1}$)	Energy ($J \cdot mol^{-1}$)	Enthalpy ($J \cdot mol^{-1}$)	C_v ($J \cdot mol^{-1} \cdot K^{-1}$)	C_p ($J \cdot mol^{-1} \cdot K^{-1}$)	Velocity of sound ($m \cdot s^{-1}$)	Phase region
365.0	3.0	3.370	−12.5	−3917.6	−2794	1716			2
367.0	3.0	3.509	−10.9	−3330.6	−2161	1388			2
369.0	3.0	3.653	−9.2	−2724.5	−1507	1028			2
371.0	3.0	3.794	−7.7	−2154.6	−890	133	834	95.4	1
372.0	3.0	3.844	−7.3	−2023.9	−743	129	717	96.9	1
373.0	3.0	3.893	−7.0	−1895.3	−598	128	642	97.9	1
374.0	3.0	3.942	−6.6	−1767.8	−454	127	584	98.8	1
375.0	3.0	3.991	−6.3	−1640.9	−311	127	539	99.6	1
376.0	3.0	4.039	−6.0	−1514.5	−168	126	502	100.5	1
377.0	3.0	4.087	−5.6	−1388.6	−26	126	471	101.3	1
379.0	3.0	4.183	−5.0	−1137.7	256	125	423	103.0	1
381.0	3.0	4.278	−4.3	−888.0	538	125	387	104.7	1
383.0	3.0	4.372	−3.7	−639.1	818	124	359	106.3	1
385.0	3.0	4.465	−3.0	−391.0	1097	124	336	108.0	1
390.0	3.0	4.697	−1.4	226.4	1792	123	295	112.1	1
395.0	3.0	4.926	0.1	839.7	2482	122	267	116.3	1
400.0	3.0	5.153	1.7	1448.2	3166	121	246	120.3	1
405.0	3.0	5.379	3.2	2051.4	3844	120	230	124.3	1
410.0	3.0	5.602	4.6	2648.4	4516	119	217	128.2	1
415.0	3.0	5.824	6.1	3238.3	5180	117	206	132.0	1
420.0	3.0	6.043	7.5	3820.4	5835	116	196	135.7	1
425.0	3.0	6.261	8.8	4394.0	6481	114	188	139.4	1
430.0	3.0	6.477	10.1	4958.4	7117	112	180	142.9	1
435.0	3.0	6.690	11.4	5513.1	7743	110	172	146.4	1
440.0	3.0	6.901	12.7	6057.7	8358	108	166	149.7	1
445.0	3.0	7.110	13.9	6591.8	8962	106	159	153.0	1
450.0	3.0	7.316	15.1	7114.9	9553	104	153	156.1	1

365.0	4.0	3.370	−18.1	−5704.2	−4862	1668			2
367.0	4.0	3.509	−16.7	−5198.9	−4322	1501			2
369.0	4.0	3.653	−15.3	−4679.0	−3766	1339			2
371.0	4.0	3.803	−13.9	−4136.2	−3186	1170			2
372.0	4.0	3.880	−13.1	−3851.5	−2882	1082			2
373.0	4.0	3.959	−12.3	−3552.2	−2562	992			2
374.0	4.0	4.038	−11.5	−3257.8	−2248	149	6113	87.8	1
375.0	4.0	4.108	−11.1	−3112.1	−2085	143	3045	89.4	1
376.0	4.0	4.176	−10.7	−2971.5	−1927	139	2076	90.8	1
377.0	4.0	4.244	−10.4	−2834.0	−1773	136	1589	92.0	1
379.0	4.0	4.378	−9.7	−2564.9	−1470	133	1098	94.3	1
381.0	4.0	4.512	−9.0	−2301.1	−1173	131	850	96.5	1
383.0	4.0	4.644	−8.3	−2040.8	−880	129	701	98.6	1
385.0	4.0	4.776	−7.6	−1783.1	−589	128	602	100.7	1
390.0	4.0	5.104	−6.0	−1146.8	129	126	456	105.8	1
395.0	4.0	5.430	−4.4	−519.0	839	125	377	110.7	1
400.0	4.0	5.755	−2.8	102.0	1541	124	328	115.6	1
405.0	4.0	6.078	−1.3	716.5	2236	122	294	120.4	1
410.0	4.0	6.401	0.2	1324.5	2925	121	268	125.1	1
415.0	4.0	6.722	1.7	1925.8	3606	120	249	129.7	1
420.0	4.0	7.042	3.1	2519.8	4280	118	233	134.2	1
425.0	4.0	7.361	4.5	3106.3	4946	117	220	138.6	1
430.0	4.0	7.678	5.8	3684.8	5604	115	209	142.9	1
435.0	4.0	7.993	7.1	4255.0	6253	113	199	147.0	1
440.0	4.0	8.307	8.4	4816.5	6893	111	190	151.1	1
445.0	4.0	8.618	9.7	5369.0	7523	110	182	155.1	1
450.0	4.0	8.927	10.9	5912.3	8144	108	175	159.0	1

Table IV. *(Continued)*

Temp. (K)	Density ($mol \cdot L^{-1}$)	Pressure (MPa)	Entropy ($J \cdot mol^{-1} \cdot K^{-1}$)	Energy ($J \cdot mol^{-1}$)	Enthalpy ($J \cdot mol^{-1}$)	C_v ($J \cdot mol^{-1} \cdot K^{-1}$)	C_p ($J \cdot mol^{-1} \cdot K^{-1}$)	Velocity of sound ($m \cdot s^{-1}$)	Phase region
365.0	5.0	3.370	−21.5	−6776.2	−6102	1356			2
367.0	5.0	3.509	−20.3	−6319.9	−5618	1258			2
369.0	5.0	3.653	−19.0	−5851.7	−5121	1170			2
371.0	5.0	3.803	−17.7	−5365.4	−4605	1088			2
372.0	5.0	3.880	−17.0	−5111.8	−4336	1052			2
373.0	5.0	3.959	−16.3	−4846.7	−4055	1025			2
374.0	5.0	4.040	−15.5	−4557.6	−3750	1059			2
375.0	5.0	4.123	−14.9	−4331.4	−3507	157	15880	80.8	1
376.0	5.0	4.206	−14.5	−4181.2	−3340	146	5515	85.0	1
377.0	5.0	4.290	−14.1	−4038.4	−3180	140	3224	87.7	1
379.0	5.0	4.457	−13.4	−3763.6	−2872	135	1733	91.8	1
381.0	5.0	4.626	−12.7	−3496.7	−2572	132	1188	95.2	1
383.0	5.0	4.795	−12.0	−3234.6	−2276	130	911	98.3	1
385.0	5.0	4.964	−11.4	−2975.8	−1983	129	745	101.2	1
390.0	5.0	5.391	−9.7	−2338.4	−1260	126	527	107.9	1
395.0	5.0	5.820	−8.1	−1710.5	−547	125	420	114.3	1
400.0	5.0	6.251	−6.5	−1089.5	161	124	357	120.4	1
405.0	5.0	6.684	−5.0	−474.6	862	122	315	126.3	1
410.0	5.0	7.118	−3.5	134.2	1558	121	285	132.0	1
415.0	5.0	7.553	−2.1	737.0	2248	120	263	137.5	1
420.0	5.0	7.988	−0.6	1333.5	2931	119	245	142.9	1
425.0	5.0	8.424	0.8	1923.3	3608	117	231	148.2	1
430.0	5.0	8.860	2.1	2506.1	4278	116	219	153.3	1
435.0	5.0	9.296	3.5	3081.7	4941	114	208	158.3	1
440.0	5.0	9.731	4.8	3649.7	5596	113	199	163.2	1
445.0	5.0	10.165	6.0	4209.9	6243	111	191	167.9	1
450.0	5.0	10.597	7.3	4762.1	6882	110	184	172.6	1

365.0	6.0	3.370	−23.8	−7490.9	−6929	1087			2
367.0	6.0	3.509	−22.6	−7067.2	−6482	1025			2
369.0	6.0	3.653	−21.5	−6633.5	−6025	973			2
371.0	6.0	3.803	−20.2	−6184.9	−5551	929			2
372.0	6.0	3.880	−19.6	−5952.0	−5305	913			2
373.0	6.0	3.959	−19.0	−5709.7	−5050	909			2
374.0	6.0	4.041	−18.3	−5454.1	−4781	143	5766	82.7	1
375.0	6.0	4.139	−17.9	−5314.9	−4625	136	2471	88.9	1
376.0	6.0	4.240	−17.6	−5180.4	−4474	133	1666	93.0	1
377.0	6.0	4.343	−17.2	−5048.6	−4325	131	1283	96.3	1
379.0	6.0	4.551	−16.5	−4789.6	−4031	128	905	101.6	1
381.0	6.0	4.762	−15.8	−4534.6	−3741	127	715	106.2	1
383.0	6.0	4.977	−15.2	−4282.3	−3453	126	601	110.3	1
385.0	6.0	5.193	−14.5	−4031.8	−3166	125	524	114.2	1
390.0	6.0	5.742	−12.9	−3411.0	−2454	124	410	122.9	1
395.0	6.0	6.300	−11.4	−2796.0	−1746	123	347	130.9	1
400.0	6.0	6.865	−9.8	−2185.5	−1041	122	307	138.4	1
405.0	6.0	7.436	−8.3	−1579.2	−340	121	279	145.5	1
410.0	6.0	8.011	−6.8	−977.4	358	120	258	152.3	1
415.0	6.0	8.591	−5.4	−380.3	1052	119	242	158.9	1
420.0	6.0	9.173	−4.0	211.8	1741	118	229	165.3	1
425.0	6.0	9.758	−2.6	798.5	2425	117	218	171.5	1
430.0	6.0	10.345	−1.2	1379.3	3103	116	208	177.5	1
435.0	6.0	10.934	0.1	1953.9	3776	114	200	183.3	1
440.0	6.0	11.524	1.4	2522.1	4443	113	193	189.0	1
445.0	6.0	12.114	2.7	3083.4	5102	112	186	194.6	1
450.0	6.0	12.705	3.9	3637.8	5755	110	180	200.1	1

Table IV. *(Continued)*

Temp. (K)	Density ($mol \cdot L^{-1}$)	Pressure (MPa)	Entropy ($J \cdot mol^{-1} \cdot K^{-1}$)	Energy ($J \cdot mol^{-1}$)	Enthalpy ($J \cdot mol^{-1}$)	C_v ($J \cdot mol^{-1} \cdot K^{-1}$)	C_p ($J \cdot mol^{-1} \cdot K^{-1}$)	Velocity of sound ($m \cdot s^{-1}$)	Phase region
365.0	7.0	3.370	−25.4	−8001.3	−7520	883			2
367.0	7.0	3.509	−24.3	−7601.0	−7100	843			2
369.0	7.0	3.653	−23.2	−7191.9	−6670	810			2
371.0	7.0	3.803	−22.1	−6770.2	−6227	785			2
372.0	7.0	3.913	−21.6	−6611.7	−6053	122	625	115.1	1
373.0	7.0	4.046	−21.3	−6489.9	−5912	122	556	118.8	1
374.0	7.0	4.181	−21.0	−6368.6	−5771	121	507	122.0	1
375.0	7.0	4.317	−20.7	−6247.6	−5631	121	470	125.1	1
376.0	7.0	4.455	−20.3	−6126.8	−5490	121	440	127.9	1
377.0	7.0	4.593	−20.0	−6006.3	−5350	120	416	130.6	1
379.0	7.0	4.873	−19.4	−5765.8	−5070	120	378	135.6	1
381.0	7.0	5.157	−18.8	−5525.8	−4789	120	350	140.2	1
383.0	7.0	5.444	−18.1	−5286.0	−4508	120	328	144.6	1
385.0	7.0	5.733	−17.5	−5046.5	−4227	120	311	148.7	1
390.0	7.0	6.467	−16.0	−4448.4	−3525	120	279	158.3	1
395.0	7.0	7.214	−14.4	−3851.5	−2821	119	257	167.2	1
400.0	7.0	7.970	−12.9	−3256.0	−2117	119	240	175.6	1
405.0	7.0	8.736	−11.5	−2662.5	−1415	118	228	183.7	1
410.0	7.0	9.508	−10.0	−2071.6	−713	118	217	191.4	1
415.0	7.0	10.288	−8.6	−1483.8	−14	117	209	198.8	1
420.0	7.0	11.072	−7.2	−899.7	682	116	201	206.0	1
425.0	7.0	11.862	−5.8	−319.8	1375	116	195	213.0	1
430.0	7.0	12.656	−4.5	255.4	2063	115	189	219.8	1
435.0	7.0	13.453	−3.2	825.4	2747	113	184	226.4	1
440.0	7.0	14.253	−1.9	1390.0	3426	112	179	232.9	1
445.0	7.0	15.056	−0.6	1948.7	4100	111	174	239.3	1
450.0	7.0	15.861	0.6	2501.3	4767	110	170	245.5	1

365.0	8.0	3.370	−26.6	−8384.2	−7963	732			2
367.0	8.0	3.738	−26.0	−8158.4	−7691	112	290	168.0	1
369.0	8.0	4.112	−25.4	−7933.1	−7419	113	275	173.5	1
371.0	8.0	4.491	−24.8	−7707.0	−7146	113	264	178.6	1
372.0	8.0	4.681	−24.5	−7593.6	−7008	113	259	181.0	1
373.0	8.0	4.873	−24.2	−7480.0	−6871	114	254	183.4	1
374.0	8.0	5.066	−23.9	−7366.2	−6733	114	250	185.7	1
375.0	8.0	5.260	−23.6	−7252.3	−6595	114	246	188.0	1
376.0	8.0	5.454	−23.3	−7138.1	−6456	114	243	190.2	1
377.0	8.0	5.649	−23.0	−7023.8	−6318	114	239	192.4	1
379.0	8.0	6.042	−22.4	−6794.6	−6039	115	233	196.7	1
381.0	8.0	6.438	−21.7	−6564.8	−5760	115	228	200.8	1
383.0	8.0	6.836	−21.1	−6334.5	−5480	115	224	204.8	1
385.0	8.0	7.237	−20.5	−6103.7	−5199	116	219	208.8	1
390.0	8.0	8.250	−19.0	−5524.9	−4494	116	211	218.2	1
395.0	8.0	9.275	−17.6	−4944.5	−3785	116	203	227.3	1
400.0	8.0	10.313	−16.1	−4363.5	−3074	116	197	236.0	1
405.0	8.0	11.360	−14.7	−3782.9	−2363	116	192	244.5	1
410.0	8.0	12.417	−13.2	−3203.4	−1651	116	188	252.7	1
415.0	8.0	13.482	−11.8	−2625.8	−940	115	183	260.7	1
420.0	8.0	14.555	−10.5	−2050.8	−231	115	179	268.5	1
425.0	8.0	15.635	−9.1	−1479.0	475	114	176	276.1	1
430.0	8.0	16.720	−7.8	−911.0	1179	113	172	283.6	1
435.0	8.0	17.811	−6.5	−347.2	1879	112	169	290.9	1
440.0	8.0	18.906	−5.2	211.8	2575	111	166	298.1	1
445.0	8.0	20.006	−4.0	765.9	3267	110	163	305.2	1
450.0	8.0	21.110	−2.7	1314.6	3953	109	160	312.2	1

Table V. Calculated Saturation Properties

Temp. (K)	Liquid density ($mol \cdot L^{-1}$)	Vapor density ($mol \cdot L^{-1}$)	Vapor pressure (MPa)	Latent heat ($J \cdot mol^{-1}$)
374.15	5.770	4.331	4.053	1780
374.00	5.956	4.147	4.040	2252
373.85	6.086	4.018	4.028	2587
373.70	6.191	3.915	4.016	2860
373.55	6.279	3.829	4.003	3089
373.40	6.357	3.753	3.991	3295
373.25	6.426	3.685	3.979	3479
373.10	6.490	3.624	3.967	3647
372.80	6.603	3.516	3.943	3948
372.50	6.702	3.421	3.919	4215
372.20	6.792	3.337	3.896	4456
371.90	6.873	3.261	3.872	4676
371.60	6.949	3.191	3.849	4881
371.30	7.019	3.126	3.826	5073
371.00	7.086	3.066	3.803	5253
370.70	7.148	3.009	3.780	5423
370.40	7.208	2.956	3.757	5585
370.10	7.265	2.906	3.734	5739
369.80	7.320	2.858	3.712	5888
369.50	7.372	2.813	3.690	6028
369.20	7.423	2.769	3.668	6166
368.90	7.471	2.728	3.645	6295
368.60	7.519	2.688	3.624	6422
368.30	7.565	2.649	3.602	6546
368.00	7.609	2.612	3.580	6664
367.70	7.652	2.577	3.559	6777
367.40	7.695	2.542	3.537	6891
367.10	7.736	2.509	3.516	6998
366.80	7.776	2.477	3.495	7102
366.50	7.816	2.446	3.474	7203
366.20	7.854	2.416	3.453	7300
365.90	7.892	2.387	3.432	7395
365.60	7.929	2.360	3.411	7483
365.30	7.966	2.333	3.391	7570
365.00	8.001	2.308	3.370	7649
364.70	8.037	2.284	3.350	7724

REFERENCES

1. M. O. McLinden and D. A. Didion, *ASHRAE J.* **29**(12):32 (1987).
2. J. M. Steed, *Int. J. Thermophys.* **10**:545 (1989).
3. B. Sukornick, *Int. J. Thermophys.* **10**:553 (1989).

4. L. E. Manzer, *Science* **249**:31 (1990).
5. M. O. McLinden and D. A. Didion, *Int. J. Thermophys.* **10**:563 (1989).
6. D. P. Wilson and R. S. Basu, *ASHRAE Trans.* **94** (Part 2):2095 (1988).
7. R. S. Basu and D. P. Wilson, *Int. J. Thermophys.* **10**:591 (1989).
8. Y. Kabata, S. Tanikawa, M. Uetmatsu, and K. Watanabe, *Int. J. Thermophys.* **10**:605 (1989).
9. L. A. Weber, *Int. J. Thermophys.* **10**:617 (1989).
10. H. Kubota, T. Yamashita, Y. Tanaka, and T. Makita, *Int. J. Thermophys.* **10**:629 (1989).
11. M. O. McLinden, J. S. Gallagher, L. A. Weber, G. Morrison, D. Ward, A. R. H. Goodwin, M. R. Moldover, J. W. Schmidt, H. B. Chae, T. J. Bruno, J. F. Ely, and M. L. Huber, *ASHRAE Trans.* **95** (Part 2):263 (1989).
12. C. C. Piao, H. Sato, and K. Watanabe, *ASHRAE Trans.* **96** (Part 1):132 (1990).
13. A. Saitoh, S. Nakagawa, H. Sato, and K. Watanabe, *J. Chem. Eng. Data* **35**:107 (1990).
14. Y. Maezawa, H. Sato, and K. Watanabe, *J. Chem. Eng. Data* **35**:225 (1990).
15. G. Morrison and D. K. Ward, *Fluid Phase Equil.* **62**:(in press) (1991).
16. A. R. H. Goodwin and M. R. Moldover, *J. Chem. Phys.* **93**:2741 (1990).
17. J. V. Sengers and J. M. H. Levelt Sengers, *Chem. Eng. News* **46**(10):104 (1968).
18. M. E. Fisher, in *Critical Phenomena, Vol. 186, Lecture Notes in Physics*, F. J. W. Hahne, ed. (Springer-Verlag, Berlin, 1982), p. 1.
19. J. V. Sengers and J. M. H. Levelt Sengers, *Annu. Rev. Phys. Chem.* **37**:189 (1986).
20. J. M. H. Levelt Sengers and J. V. Sengers, in *Perspectives in Statistical Physics*, H. J. Raveché, ed. (North-Holland, Amsterdam, 1981), p. 239.
21. G. Morrison and J. S. Gallagher, in *Proceedings, 1990 USNC/11R-Purdue Refrigeration Conference and 1990 ASHRAE-Purdue CFC Conference*, D. R. Tree, ed. (Purdue University, West Lafayette, IN, 1990), p. 242.
22. J. F. Nicoll and J. K. Bhattacharjee, *Phys. Rev. B* **23**:389 (1981).
23. J. F. Nicoll and P. C. Albright, *Phys. Rev. B* **31**:4576 (1985).
24. C. Bagnuls, C. Bervillier, and Y. Garrabos, *J. Phys. Lett.* **45**:L-127 (1984).
25. C. Bagnuls and C. Bervillier, *Phys. Rev. B* **32**:7209 (1985).
26. C. Bagnuls, C. Bervillier, D. I. Meiron, and B. G. Nickel, *Phys. Rev. B* **35**:3585 (1987).
27. P. C. Albright, J. V. Sengers, J. F. Nicoll, and M. Ley-Koo, *Int. J. Thermophys.* **7**:75 (1986).
28. P. C. Albright, Z. Y. Chen, and J. V. Sengers, *Phys. Rev. B* **36**:877 (1987).
29. V. Dohm, *J. Low Temp. Phys.* **69**:51 (1987).
30. R. Schloms and V. Dohm, *Europhys. Lett.* **3**:413 (1987).
31. R. Schloms and V. Dohm, *Nuclear Phys. B* **328**:639 (1989).
32. Z. Y. Chen, P. C. Albright, and J. V. Sengers, *Phys. Rev. A* **41**:3161 (1990).
33. Z. Y. Chen, A. Abbaci, S. Tang, and J. V. Sengers, *Phys. Rev. A* **42**:4470 (1990).
34. J. V. Sengers and J. M. H. Levelt Sengers, in *Progress in Liquid Physics* (Wiley, New York, 1978), p. 103.
35. J. F. Nicoll, *Phys. Rev. A* **24**:2203 (1981).
36. A. J. Liu and M. E. Fisher, *Physica A* **136**:35 (1989).
37. F. C. Zhang and R. K. P. Zia, *J. Phys.* **15**:3301 (1982).
38. J. C. Le Guillou and J. Zinn-Justin, *J. Phys.* **48**:19 (1987).
39. Z. Y. Chen, A. Abbaci, and J. V. Sengers, in *Properties of Water and Steam: Proceedings of the 11th International Conference*, M. Píchal and O. Šifner, eds. (Hemisphere, New York, 1990), p. 168.
40. J. M. H. Levelt Sengers, B. Kamgar-Parsi, F. W. Balfour, and J. V. Sengers, *J. Phys. Chem. Ref. Data* **12**:1 (1983).
41. J. V. Sengers and J. M. H. Levelt Sengers, *Int. J. Thermophys.* **5**:195 (1984).

42. P. C. Albright, T. J. Edwards, Z. Y. Chen, and J. V. Sengers, *J. Chem. Phys.* **87**:1717 (1987).
43. H. J. R. Guedes and J. A. Zollweg, Submitted for publication.
44. H. Chaar, M. R. Moldover, and J. W. Schmidt, *J. Chem. Phys.* **85**:418 (1986).
45. M. R. Moldover and J. C. Rainwater, *J. Chem. Phys.* **88**:7772 (1988).
46. J. S. Rowlinson and B. Widom, *Molecular Theory of Capillarity* (Clarendon, Oxford, 1982).
47. H. B. Chae, J. W. Schmidt, and M. R. Moldover, *J. Chem. Eng. Data* **35**:6 (1990).
48. G. Morrison and M. O. McLinden, *Application of a Hard Sphere Equation of State to Refrigerants and Refrigerant Mixtures*, NBS Technical Note 1226 (U.S. Government Printing Office, Washington, DC), 1986.
49. G. Morrison, Personal communication (1990).
50. J. M. H. Levelt Sengers, B. Kamgar-Parsi, and J. V. Sengers, *J. Chem. Eng. Data* **28**:354 (1983).